Waypoint Navigation with Position and Heading Control using Complex Vector Fields for an Ackermann Steering Autonomous Vehicle

Tommie J. Liddy and Tien-Fu Lu
School of Mechanical Engineering; The University of Adelaide
tommie.liddy@adelaide.edu.au; tien-fu.lu@adelaide.edu.au

Abstract

Vector field (otherwise known as force vector or force field) navigation has been used in mobile robotics primarily for goal oriented navigation and obstacle avoidance. At the most basic level the vector field consists of attractive forces, goals, and repulsive forces, usually objects. Both attractive and repulsive forces are usually characterised as point forces. The shortfall of this characterisation is that there is no way of controlling the heading of the mobile robot as it reaches the goal position. In this paper various methods of altering the goal vector field will be looked at. These methods include investigating clustered attractive and repulsive forces as well as introducing rotational and line based forces. This investigation was run using a simulated model of an Ackermann steering vehicle. Results indicated that a complex vector field approach was able to give position and heading control at waypoints with the chosen simulated vehicle.

1 Introduction

The aim of this study was to produce a robust navigation method that was able to be used with an Ackermann steering vehicle to give position and heading control. A waypoint navigation method was desired where free motion was allowed between waypoints and control of the vehicles position and heading was required at waypoint [Borenstein and Koren, 1989; Yang *et al.*, 2005]. Unlike skid steer robots[Reister and Pin, 1994; Yang *et al.*, 2005], the ability to control the heading of a front wheel steer vehicle [Spenko *et al.*, 2004] as it reaches final or intermediate waypoints is important since corrections can not be made on the spot. The following study shows how position and heading control can be achieved by combining simple elements of a vector field to produce a complex vector field used for navigation.

Vector field navigation consists of two common approaches. One is to us a grid placed over an environment [Kim *et al*, 1999] where environmental variables such as goals and obstacles are then used to produce resultant vector forces at each point on the grid. The other approach is to use the same environmental variables acting directly on the vehicle travelling through the environment [Borenstein and Koren, 1989]. For the first of these two methods the vector force throughout the grid is calculated before navigation begins, whereas the second method recalculates the vector force acting on the vehicle at regular intervals. The second approach is better suited for dynamic environments and since that is the end goal of this research the resultant force method has been adopted for this study. The resultant force method developed in this study combines various vector field components such as, point force vector fields [Borenstein and Koren, 1989], rotational fields [Kim *et al.*, 1999] and line force [Loizou *et al.*, 2003] to control an autonomous vehicle.

The autonomous vehicle used throughout this study was a geometric model of a four wheeled quad bike. This vehicle was used for the model so as to tie in with future research. Therefore the quad bike model has taken on the dimensions and constraints of the physical vehicle.

2 Simulated vehicle model and complex vector field

As all experiments have been done in a simulation environment a model for the autonomous vehicle was required. An Ackermann steering vehicle was chosen as the robotic model. The vehicle was based on a Honda quad bike which will be used for real world tests building upon the results obtained through simulation. The environment the simulated vehicle travelled through was a flat plane (the X-Y plane). Waypoints were created in this environment for the vehicle to navigate to, these waypoints were considered to be points in the X-Y plane with a heading also in the X-Y plane, about the Z-axis, from -180 degrees to +180 degrees. To navigate through these waypoints the simulated vehicle was affected by various vector field components in combination, called a complex vector field.

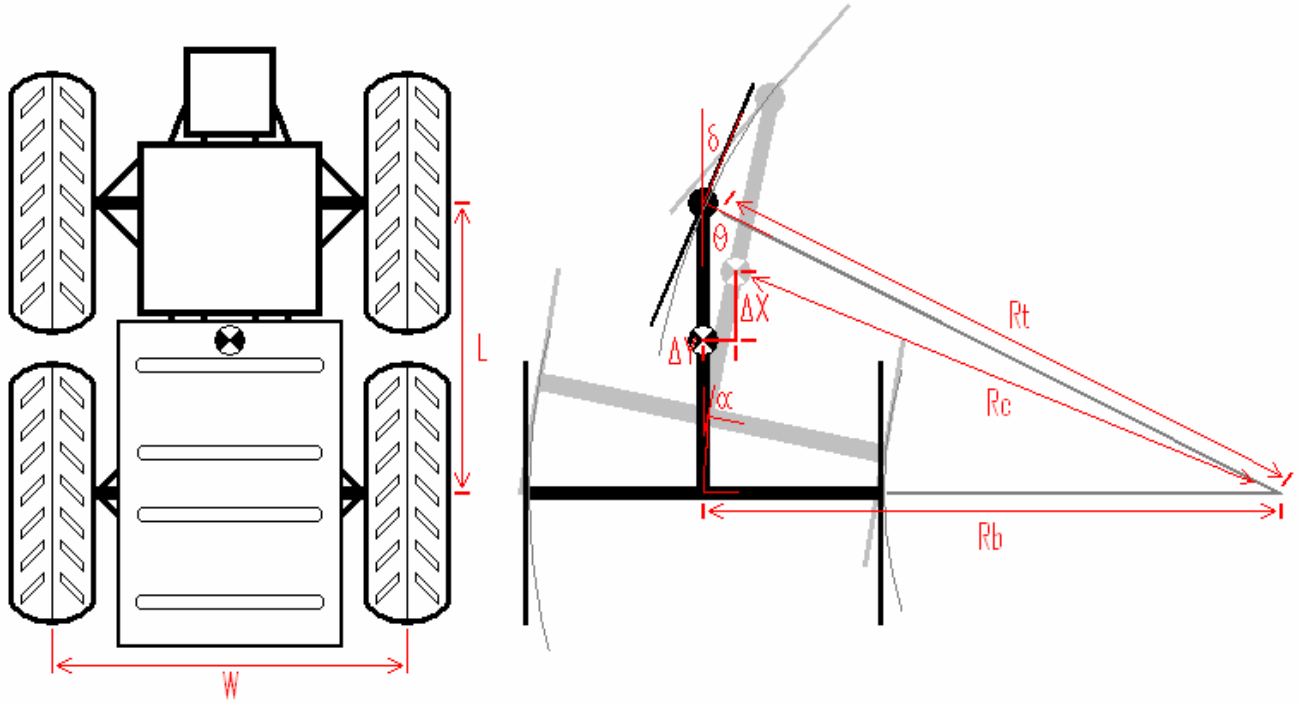

Figure 1: Geometric model Derived from a front wheel steering quad bike

2.1 Vehicle model

The vehicle model developed was a geometric representation of an Ackermann steering vehicle. To model the steering mechanism the two front wheels of the vehicle were simplified to one wheel located in the middle of front axle (as shown in Figure 1). An assumption was made that all of the wheels were able to travel in an arc centred about the same point and that over a short time span this arc was at a constant radius. With these simplification and assumptions a mathematical model was developed for the simulated vehicle. The mathematical model used the geometry of the Honda quad bike to relate steering angle and velocity to position shift and change in heading.

For the simulation environment the vehicle was assumed to be a point in the X-Y plane with a heading about the Z-axis, this point corresponds to the centre of the vehicle shown in Figure 1. To determine the change in position and heading based on the vehicles instantaneous velocity (V), front steering angle (δ) and the time step between the current reading and the next expected reading (Δt), Equations 1 to 5 were developed, where Rt, Rb and Rc are shown in Figure 1 and D represents the distance travelled over the time step.

$$\theta = 90 - \delta \quad (1)$$

$$Rt = \frac{L}{Cos(\theta)} \quad (2)$$

$$Rb = \sqrt{Rt^2 - L^2} \quad (3)$$

$$D = \Delta t * V \quad (4)$$

$$\alpha = \frac{D}{Rb} \quad (5)$$

The change in position with reference to the current vehicles reference frame was then calculated from Equations 6 and 7.

$$\Delta X = Rc * Sin(\alpha) \quad (6)$$

$$\Delta Y = Rc(1 - Cos(\alpha)) \quad (7)$$

Conversely, to find the steering angle based on the desired change in heading (α), velocity (V) and time step (Δt), the equations can be reversed as shown by equations 8 to 12.

$$D = \Delta t * V \quad (8)$$

$$Rb = \frac{D}{\alpha} \quad (9)$$

$$Rt = \sqrt{Rb^2 + L^2} \quad (10)$$

$$\theta = Arc\cos\left(\frac{L}{Rt}\right) \quad (11)$$

$$\delta = 90 - \theta \quad (12)$$

The vector field used for navigation determined the desired heading of the vehicle. From the desired heading Equations 8 to 12 were used to determine the steering angle the vehicle required. This required steering angle was then amended according to the physical limitations of the modelled quad bike, such as maximum and minimum position as well as turning speed. The amended steering angle was then used in Equations 1 to 7 to produce the vehicles change in position and heading.

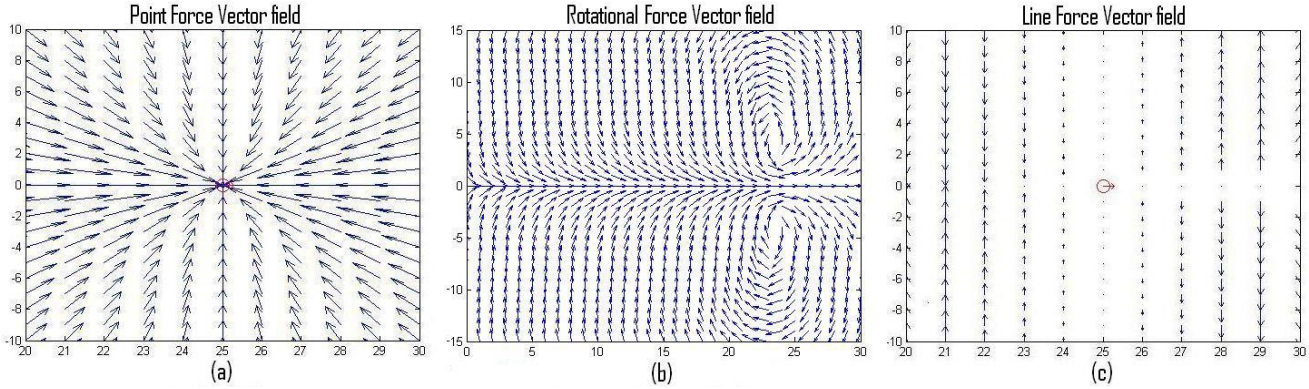

Figure 2: (a) Point force vector field component; (b) Rotational force vector field component; (c) Line force vector field component; (d) Force magnitude trend.

2.2 Vector field components

Vector field navigation typically consists of attractive and repulsive forces being applied to a body, in this case a simulated vehicle, to direct it to a desired location [Borenstein and Koren, 1989; Kim *et al.*, 1999]. The attractive force is most commonly created by waypoints which represent the desired destination or a set of intermediate points which must be reached. Each of the vector field components used for the complex vector field were likewise centred about waypoints.

The complex vector field that was used during simulation consisted of a combination of various vector field components. The components used were point forces (Figure 2(a)), rotational forces (Figure 2(b)) and line forces (Figure 2(c)). Each vector force component comprises of a set of two functions, one determining the X-axis component of the force the other determining the Y-axis component. Both components are functions of the vehicles position relative to the waypoint measured in the reference frame of the waypoint. Equations 13 and 14 are an example of the X-axis and Y-axis force function used to create the vector field shown in Figure 2(a), where Xv_{wp} and Yv_{wp} represent the X-axis and Y-axis distance from the vehicle to the waypoint in the reference frame of the waypoint.

$$Fx = \frac{Xv_{WP}}{\sqrt{Xv_{WP}^2 + Yv_{WP}^2}} \tag{13}$$

$$Fy = \frac{Yv_{WP}}{\sqrt{Xv_{WP}^2 + Yv_{WP}^2}} \tag{14}$$

The vector field components are characterised by their waypoint, for example, Figure 2(a) is an attractive point force which is centred about the waypoint. It is also possible to centre components away from the waypoint with an X or Y axis offset as shown in Figure 2(b). The waypoints define three terms, the goal position, the goal heading and the goal line, which is a vector that passes through the goal position along the goal heading.

2.3 Producing a complex vector field

The base of the complex vector field was chosen as an attractive point force with constant force magnitude at any distance (Equations 13 and 14), similar to that used in Borenstein and Koren [1989]. With the front wheel steering vehicle this vector field was still able to produce results where the desired position was reached, however there was no control over the vehicle's heading at the waypoint. To achieve nominal heading control a line vector field was added to the original vector field (Equations 15 and 16). These two simple fields were able to give position and heading control where the vehicle's starting position was within ±60 degrees of the goal line. Outside this range, it was impossible to obtain both position and heading control.

$$Fx = 0 \tag{15}$$

$$Fy = Min\left(1, Abs\left(Yv_{WP}\right)\right) * \ldots \ldots Min\left(1, Abs\left(Xv_{WP}\right)\right) * Sign\left(Yv_{WP}\right) \tag{16}$$

The next step in developing the complex vector field was to improve the results for starting positions outside of the ±60 degrees range. To do this multiple vector field components were added to the complex vector field. A pair of rotational vector field components coupled with repulsive vector field components was added above and below the goal position. The rotational vector fields were clockwise below the waypoint and counter-clockwise above the waypoint, similar to that of Figure 2(b). Equations 17 and 18 were used to calculate the rotational vector field, since the rotational vectors were desired to be above and below the waypoint an offset in the Y-axis of the waypoint reference frame were included in the calculations

$$Fx = \frac{\mp\left(Yv_{WP} \mp Offset\right)}{Xv_{WP}^2 + \left(Yv_{WP} \mp Offset\right)^2} \tag{17}$$

$$Fy = \frac{\pm Xv_{WP}}{Xv_{WP}^2 + \left(Yv_{WP} \mp Offset\right)^2} \tag{18}$$

The results from the point, line and rotation complex vector field show that reaching the desired position was possible for all starting positions, with reasonable heading control as indicated by the examples shown in Figure 3.

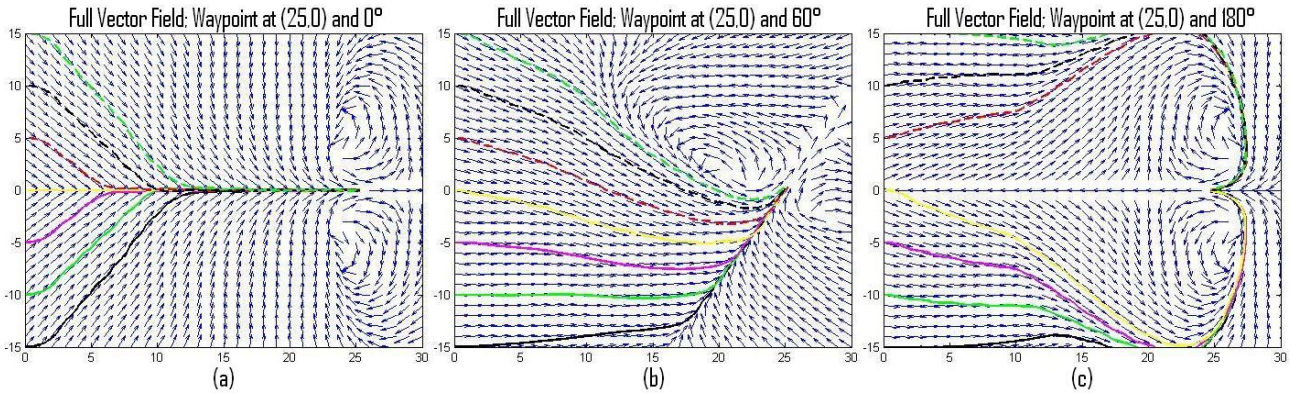

Figure 3: Multiple simulated vehicle paths with different starting points and various goal headings of (a) 0 degrees; (b) 60 degrees; (c) 180 degrees (dimensions in metres).

2.4 Simulated vehicle paths

The Simulated vehicle paths were created by using the geometric model of the vehicle to determine how it would react to the complex vector field. The vector field produced a force measured at the centre of the vehicle, this force had direction and magnitude. The direction of the force indicated the desired heading of the vehicle whereas the magnitude corresponded to the desired velocity. In addition to this the simulation system was given a realistic time step (Δt) of 0.2 seconds to represent one cycle in the computation of the physical system. This figure was reached by analysing the time constraints associated with the sensor and actuator feedback and computational costs incurred by the autonomous quad bike currently being developed to continue on the research conducted in simulation. Geometric constraints were applied to the front wheel steering mechanism limiting the steering angle and change in angle, also taken from the autonomous quad bike.

Both the simulator vehicle and the waypoint were given a position and heading in a global reference frame. Each time step the vehicle position and heading was recalculated producing a simulated vehicle path. The simulated vehicle path was terminated once the vehicle reached the final waypoint. This was considered to have happened when two conditions where achieved, firstly the vehicle had come within half a metre of the goal position and secondly the distance from the vehicle to the goal position had increased. By using these two conditions it was possible to attain the closest point the vehicle came to the waypoint once within the half metre range. This point was recorded as the vehicles final position and heading. For the tests preformed in Section 3 a limit of a thousand time steps were used to determine if the simulation vehicle failed to reach the waypoint.

3 Complex vector field results

With any one of the vector field components alone it was impossible to achieve position and heading control at waypoints in a reliable fashion. However, by combining multiple components into one vector field it was possible to produce results where position and heading control was achievable. This could be seen in Figure 3, which shows a small set of the results obtained. Each plot in Figure 3 shows seven separate vehicle paths with different initial positions and the same goal position and heading. These results indicate graphically that the simulated vehicle was able to reach the waypoint with position and heading control by using the complex vector field.

To gauge the accuracy of the complex vector field navigation method a set of tests were run which varied the initial heading of the vehicle and the goal heading of the waypoint. These tests involved altering the initial heading of the vehicle and the goal heading at the waypoint. The initial heading was varied from -170 degrees to +180 degrees and the goal heading was varied from 0 degrees to 350 degrees, both in increments of 10 degrees. The initial position of the vehicle was set to (0,0) and the goal position was set to (25,0) in the global reference frame. Due to the physical restraints of the simulated vehicle it was possible for the vehicle position to move 20cm and the vehicle heading to change by up to 3.43 degrees per time stamp. From these constraints it was decided that a position accuracy of less than 10cm would be considered satisfactory, while a heading accuracy of within 3.5 degrees would also be considered satisfactory.

By using the complex vector field created in Section 3.1 the results displayed in Figure 4 were obtained by measuring the final position and heading of the simulated vehicle. The distance from the final position to the goal position and the absolute difference in heading and goal heading were averaged over the vehicles initial heading. From the results shown Figure 4(a) it could be seen that the distance form the final position to the goal position was between 15cm and 17.5cm. Similarly the results in Figure 4(b) show that the difference between the final heading and the goal heading was between 4.7 and 5.5 degrees. Both of these results failed to meet that which would be considered satisfactory. Although unsatisfactory the results still indicate that the navigation method was close to producing the desired accuracy.

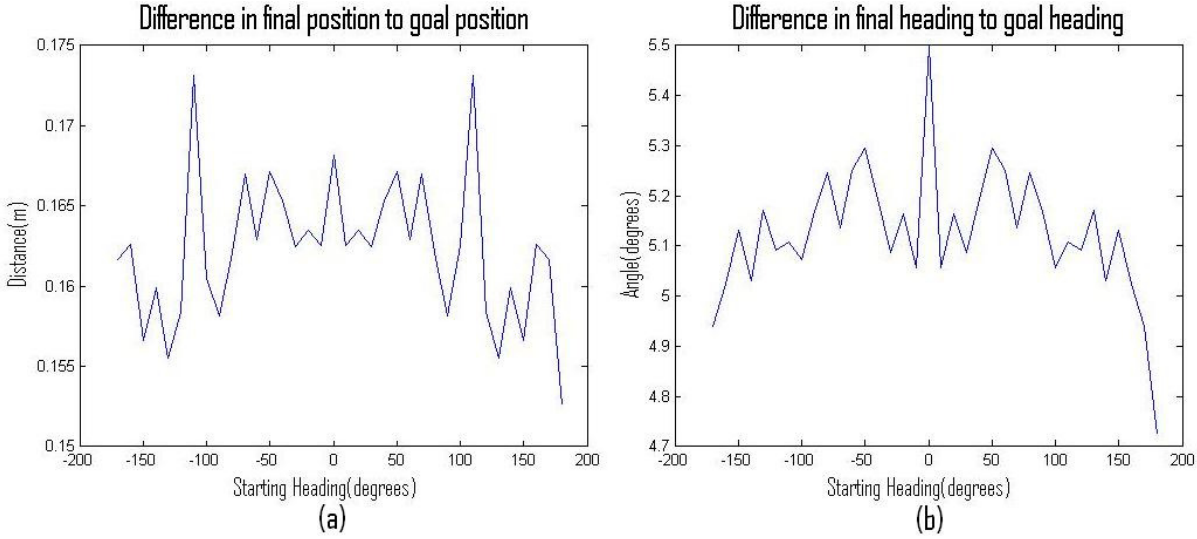

Figure 4: Averaged results over the vehicles initial heading; (a) Distance from final position to goal; (b) Difference between final heading and goal heading.

3.1 Improving the accuracy of the heading control

The results obtained from the tests run in Section 3 indicate that heading and position control was possible with the complex vector field. Both position and heading accuracy obtained through these tests did not reach a level that would be considered satisfactory. By analysing the results of individual simulated vehicle paths, similar to those shown in Figure 3, it could be seen that when the simulated vehicle crossed the waypoint it was often in the act of turning. Also, if the simulated vehicle approached the goal line with the steering mechanism at full lock the simulated path would sometimes overshot it and required a small distance to settle in to a straight line. The lateness of the simulated vehicles turning as well as the settling distance was responsible for a portion of the inaccuracy of the results in Section 3.2.

3.2 Complex vector field with a secondary waypoint

To overcome the inaccuracy caused by the overshoot and to allow for the settling distance when required a secondary waypoint was added for each goal position and heading. The secondary waypoint was put along the goal line 2m behind the goal position. From the results obtained in Section 3.2 the simulated vehicle should pass through the secondary waypoint with the accuracy shown in Figure 4 then travel the required 2m to the original waypoint. This measure was designed to give the simulated vehicle more time to settle as it approached the original waypoint. The affect of the secondary waypoint can be seen in Figure 5. For situations where the goal heading was equal to or less than 60 degrees the results obtained by adding the secondary waypoint were similar to those obtained using the complex vector field by itself (Figure 5(a) and 5(b)). The results obtained for situations where the desired angle was greater than 60 degrees showed a visible improvement (Figure 5(c)). To quantify this improvement the tests done in Section 3.2 were repeated.

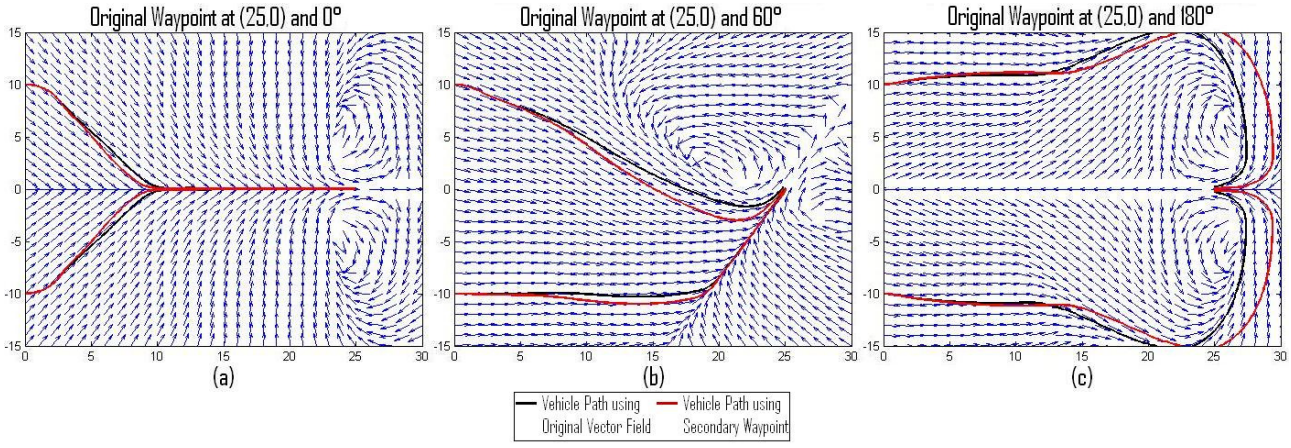

Figure 5: Simulated vehicle paths Using both the complex vector field by itself and the complex vector with the addition of the secondary waypoint with goal headings of (a) 0 degrees; (b) 60 degrees; (c) 180 degrees (dimensions in metres).

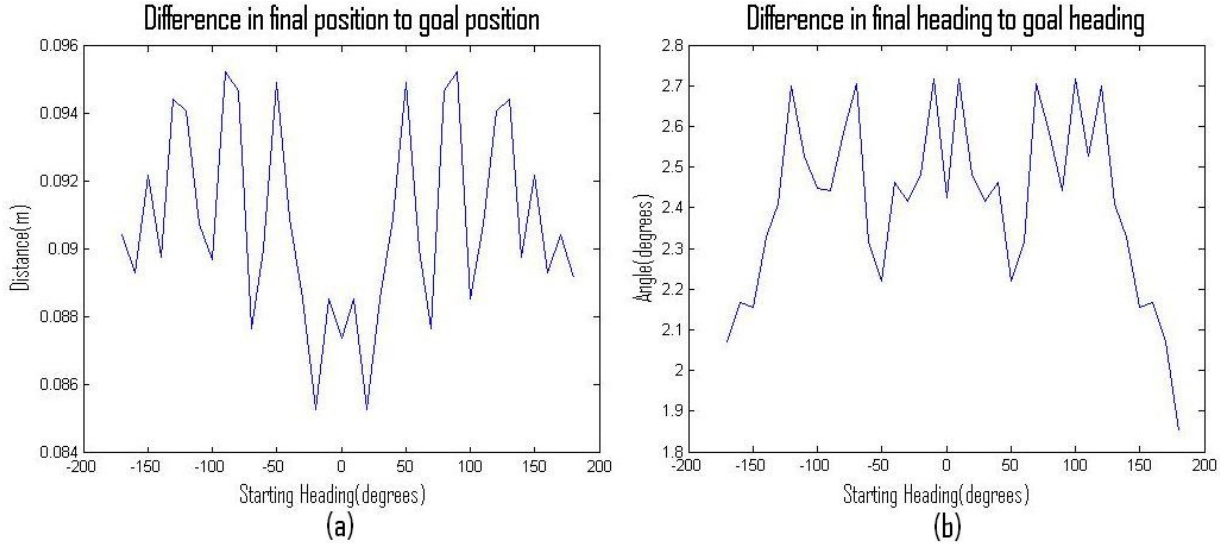

Figure 6: Averaged results over goal headings by starting angle with secondary waypoint; (a) Distance from final position to goal; (b) Difference between final heading and goal heading.

The addition of the secondary waypoint was able to produce far better results, as shown in Figure 6. By comparing these results with those from Section 3.2 the effect of adding a secondary waypoint could be seen. The position accuracy has been shown to be below 9.8cm and the heading accuracy kept below 2.8 degrees. The results obtained fall within the satisfactory range, indicating that position and heading control has been achieved. The results also indicate that the vector field navigation method could satisfactorily be implemented for a front wheel steering vehicle

5 Conclusion

Vector field navigation has been used commonly on skid steer vehicles with no minimum turning circle. For these vehicles it has been a simple matter of turning on the spot when the goal position had been reached to achieve a desired heading. However, if an Ackermann steering vehicle was being used this was not possible and therefore another approach was required. Through an iterative, observation based simulation approach it has been shown that with multiple vector field components it was possible to obtain a complex vector field which was able to produce position and heading control for an Ackermann steer vehicle.

Although the accuracy of this method was not within satisfactory limits it was near enough to warrant further development. This was done by determining the shortcomings of the original approach and looking at ways to overcome them. This was done by the addition of a secondary waypoint, which was developed mainly to improve the accuracy of the heading control. With this addition the accuracy of both the position and heading control was within previously set satisfactory limits. These results showed that this study delivered a complex vector field method which incorporated secondary waypoints for the navigation of an Ackermann steering vehicle.

References

[Borenstein and Koren, 1989] J. Borenstein and Y. Koren. Real-Time Obstacle Avoidance for Fast Mobile Robots. IEEE Transactions on Systems, Man, and Cybernetics. Vol. 19, No. 5, pp. 1179-1187, September/October 1989.

[Kim *et al.*, 1999] Yong-Jae Kim, Dong-Han Kim and Jong-Hwan Kim. Evolutionary Programming-Based Uni-vector Field Method for Fast Mobile Robot Navigation. SEAL'98, LNCS 1585, pp. 154-161, 1999.

[Loizuo *et al.*, 2003] Savvas G. Loizou, Herbert G. Tanner, Vijay Kumar and Kostas J. Kyriakopoulos. Closed Loop Motion Planning and Control for Mobile Robots in Uncertain Environments. IEEE Conference on Decision and Control, Vol. 3, pp. 2926-2931, 2003.

[Reister and Pin, 94] David B. Reister and Francois G. Pin. Time Optimal Trajectories for Mobile Robot with Two Independently Driven Wheels. International Journal of Robotics Research. Vol. 13, No. 1, pp. 38-54. 1994

[Spenko *et al.*, 2004] Matthew Spenko, Karl Iagnemma and Steven Dubowsky. High Speed Hazard Avoidance for Mobile Robots in Rough Terrain. Proceedings of SPIE, Vol. 5422, pp. 439-450, 2004.

[Yang *et al.*, 2005] Xiaoyu Yang, Mehrdad Moallem and Rajni V. Patel. A Layered Goal-Oriented Fuzzy Motion Planning Strategy for Mobile Robot Navigation. IEEE Transactions on Systems, Man, and Cybernetics-Part B. Vol.35, No. 6, December 2005.